Donor−Acceptor−Donor Tetrazines Containing a Ferrocene Unit: Synthesis, Electrochemical and Spectroscopic Properties

Izabela Janowska,[†] Fabien Miomandre,[†] Gilles Clavier,[†] Pierre Audebert,*[,†] Janusz Zakrzewski,[‡] Khuyen Hoang Thi,[§] and Isabelle Ledoux-Rak[§]

Laboratoire de Photophysique et Photochimie Supramoléculaires et Macromoléculaires, UMR CNRS 8531, Ecole Normale Supérieure de Cachan, 61 Avenue du Président Wilson, 94230 Cachan, France, Department of Organic Chemistry, University of Łódź, Narutowicza 68, 90-136 Łódź, Poland, and Laboratoire de Photonique Quantique et moléculaire, UMR CNRS 8537, Ecole Normale Supérieure de Cachan, 61 Avenue du Président Wilson, 94230 Cachan, France

Received: April 7, 2006; In Final Form: May 12, 2006

Donor−acceptor−donor tetrazines containing ferrocene moieties and phenyl unit as a π-bridge have been synthesized and characterized. UV−vis spectroscopic and cyclic voltamperometric results indicate sizable intramolecular charge transfer interactions in the ground state when the ferrocene is directly bound to the tetrazine. On the other hand, the results show reduction of the electron-donor strength of ferrocene moieties when there is a phenyl linkage. Both tetrazines display a high reduction potential. The role of ferrocenyl groups appear to be detrimental to maximize the cubic hyperpolarizability γ of tetrazines, as compared to purely organic groups such as thiophene. A possible explanation for this behavior may originate from metal-to-ligand charge transfer processes.

Introduction

Over the past decades the search for new optically and electroactive molecules as potential candidates for devices has been highly active.[1] With respect to these aims, tetrazine derivatives have appeared as promising targets because tetrazine is the most electrodeficient aromatic heterocycle of the C−N family.[2] Their strong electron affinity enhances the charge transfer in related conjugated molecules[3] leading to enhanced nonlinear optical (NLO) properties. Moreover, most tetrazines exhibit reversible electrochemical reduction, which also constitutes a useful feature for the achievement of electroswitchable NLO devices. Tetrazines possess low-lying π^* MO leading to a n−π^* transition in the visible region, which is responsible for their red color (*s*-tetrazine has a band at ca. 550 nm ($\epsilon \approx$ 830)).[2,4]

Within this topic, we have already published the synthesis and the electrochemical properties of several bisaryltetrazines.[5] However, another category of potentially interesting molecules in this domain encompasses transition metal complexes, especially those possessing a π-conjugated spacer. As such, the ferrocene (Fc) moiety represents one of the most important switchable d-donor metal center because it has demonstrated its ability to be stable in different oxidation states.[6] Several detailed studies have focused on Fc-donor−organic-acceptor metal-to-ligand charge transfer (MLCT) compounds in the context of nonlinear materials.[7−10]

We became therefore interested in the studies of electronic interactions between ferrocene and tetrazine moieties because this combination may yield unique correlated optical and electrochemical properties. In this report we present the synthesis, spectroscopic and electrochemical data for two new tetrazine based D−A−D (**4**) and D−π−A−π−D (**5**) systems containing a ferrocene entity as an electron-rich unit (**4** and **5**) and a phenyl as a π-aromatic bridge (**5**) (Figure 1). In addition, the behavior of analogous compounds featuring a cyano or a nitro group are also given for comparison purpose.

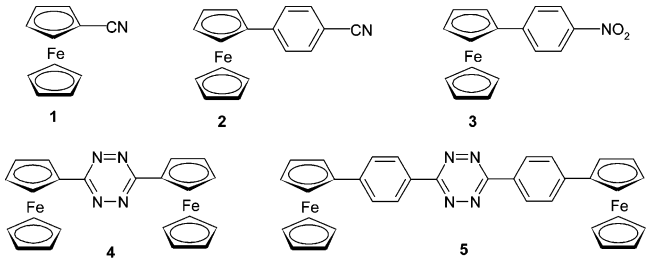

Figure 1. Formulas of *s*-tetrazines investigated (**4**, **5**) and related Fc-compounds (**1**−**3**).

SCHEME 1: Synthesis of 1,3-Bis(ferrocenylo)-*s*-tetrazine (4) and 1,3-Bis(4-ferrocenphenylo)-*s*-tetrazine (5)

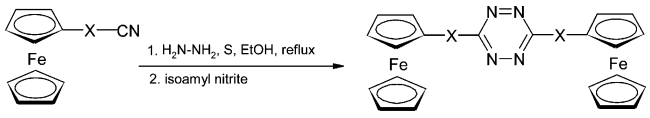

X = - (**1**), Ph (**2**) X = - (**4**), Ph (**5**)

Results and Discussion

Synthesis of 1,3-Bis(ferrocenylo)-*s*-tetrazine (4) and 1,3-Bis(4-ferrocenphenylo)-*s*-tetrazine (5). The synthetic approach followed in our work was based on a previously explored condensation of two nitrile derivatized aromatic molecules with hydrazine in the presence of sulfur[11] (Scheme 1). The reaction

[†] Laboratoire de Photophysique et Photochimie Supramoléculaires et Macromoléculaires, Ecole Normale Supérieure de Cachan.

[‡] University of Łódź.

[§] Laboratoire de Photonique Quantique et moléculaire, Ecole Normale Supérieure de Cachan.

10.1021/jp062186f CCC: $33.50
Published on Web 11/09/2006

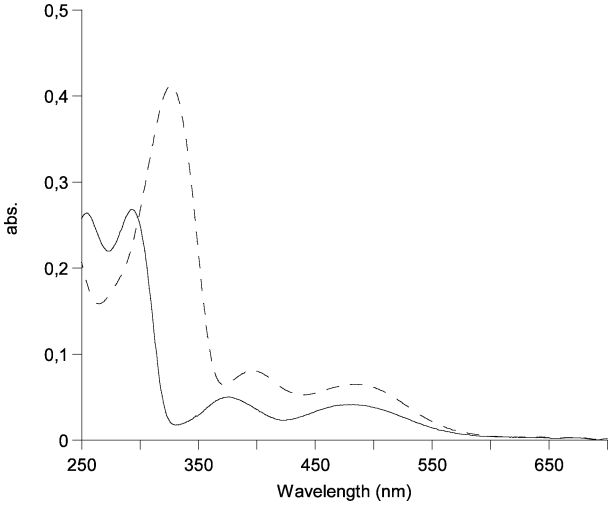

Figure 2. UV−vis absorption spectra of compounds **4** (—) and **5** (---).

conditions (closed vessel) and its mechanism has been previously studied by us.[5] The sulfur was proposed to act as an activator of the hydrazine by first producing $NH_2-NH-SH$, which then reacts on the aromatic cyano group yielding the dihydro-*s*-tetrazine, which is in turn converted to the tetrazine by oxidation with isoamyl nitrite.

The starting ferrocenylnitrile (**1**) was prepared by reaction of ferrocenecarboxaldehyde with hydroxylamine hydrochloride and triethylamine in NMP and subsequent basic treatment.[12] 4-Ferrocenylbenzonitrile (**2**) and 4-ferrocenylnitrobenzene (**3**) were prepared by a modified version of the standard diazonium reaction between ferrocenium and the diazonium salts prepared from 4-aminobenzonitrile and *p*-nitroaniline respectively.[13]

Spectroscopic Properties. The UV−vis spectra of compounds **4** and **5** were obtained in dichloromethane and are displayed in Figure 2. Electronic absorption data for **4** and **5** are collected in Table 1, along with those of the previously reported 3,6-bis(thien-2-yl)-*s*-tetrazine (**6**),[5] 3,6-bisphenylyl-*s*-tetrazine (**7**),[14] and the generic *s*-tetrazine (**8**).[2] Both tetrazines **4** and **5** show three bands, one in the UV and two bands in the visible range. These absorptions are very intense when compared to those of the other tetrazines **6**−**8**. These results indicate that large intramolecular charge transfer interactions occur. 3,6-disubstitution of tetrazine by thienyl (**6**) or phenyl groups (**7**) causes a gain in the intensity of the $\pi-\pi^*$ transition, whereas the lower $n-\pi^*$ transition is nearly unchanged, as is customary for a $n-\pi^*$ transition.[15] In the case of bisferrocenylotetrazine (**4**) and bis(ferrocenylo-4-phenylo)tetrazine (**5**), the influence of the d-metal donor center is illustrated by a high contribution of the lower energy absorption in all the electronic absorption spectra. One should take into account that the lowest energy visible band in **4** and **5** also corresponds to the metal-to-ligand charge transfer transitions from Fe(II) d-orbitals to π-orbitals of Cp−Tz (**4**) and Cp−Ph−Tz (**5**) moieties. The blue shift of the $\pi-\pi^*$ band for tetrazines **5**−**8** strongly depends on the electron-donating strength of the substituents on the tetrazine ring, whereas the red shift in compounds **4** and **5**, as compared with related derivatives **1** and **2**, indicates an increase of the acceptor force. Elongation of the conjugation π-path between the donor and acceptor moieties in **5** as compared to that in **4** facilitates the charge transfer process, resulting in a bathochromic shift and an increase in the intensity of all the bands. However, the largest shift is especially observed for the $\pi-\pi^*$ transition.

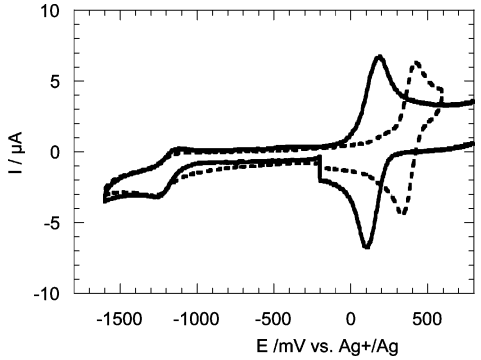

Figure 3. Cyclic voltammograms of compounds **4** (---) and **5** (—) in dichloromethane (ca. 1 mM) on glassy carbon at 0.1 V/s.

NLO Results. Third-order nonlinear susceptibilities γ of compounds **4**−**6** have been recorded in dichloromethane (Table 2).

Compounds **4** and **5** display moderate, though significant, values as compared to those of standard conjugated molecules measured in the same conditions. For example, γ values of 4,4′-cyanomethoxystilbene (4,4′-nitromethoxystilbene) do not exceed 0.5 (0.9) $\times$ 10^{-34} esu.[17]

Despite the presence of the two electron-donating ferrocene substituents in compounds **4** and **5**, their third-order susceptibility is found to be lower than that of compound **6**. This feature may be surprising, as the conjugation length in compound **5** is significantly higher than for molecule **6**. Some resonance effects could play a significant role in this enhancement of γ value for **6** as compared to **5** and **4**, as the corresponding maximum absorption wavelength λ_{max} is red-shifted by 50 nm for molecule **6** with respect to **5**. However, one could argue that ϵ and henceforth the oscillation strength is much weaker for **6**, resulting in smaller hyperpolarizability values. At the present stage of our knowledge, it may be difficult to draw any definitive conclusion about this behavior. However, it has been shown, in the case of quadratic nonlinear optical properties of metal complexes, that metal-to ligand charge tranfer processes may bring an opposite contribution with respect to that from the ligand-to-metal charge transfer, resulting in lower hyperpolarizability values,[18] for example, in the case of ruthenium as compared to zinc complexes. Therefore, it might be suggested that the nonlinear contribution from the metal-to-ligand charge transfer in ferrocene could be detrimental for the optimization of the cubic hyperpolarizability of compounds **4** and **5**, whereas in compound **6** only a $\pi-\pi^*$ transition from the thiophene to the central tetrazine moiety contributes to γ.

Electrochemical Studies. The cyclic voltamperometry studies of compounds **4** and **5** have been performed in dichloromethane solutions. The curves for the new tetrazines **4** and **5** are shown on Figure 3, where well-behaved peaks are discernible. Both compounds studied show a reversible single oxidation peak (one electron per donor unit), which is derived from removal of an electron centered on the Fc unit. As expected, the strong electron withdrawing character of the tetrazine moiety prevents the full delocalization of the positive charge between both Fc units, as would be the case in mixed valence state systems. Nevertheless, the negative oxidation potential shift from **4** to **5** indicates a rise in the highest occupied molecular orbital level due to conjugation.

In the negative potential range, compounds **4** and **5** also exhibit a reduction peak that can be attributed to the reduction of the tetrazine core. However, it can be noticed that this peak is less reversible than for previously studied tetrazine derivatives.[5]

TABLE 1: Spectroscopic Features of the Tetrazine Derivatives

compd	λ_{max1}/nm (ϵ_1/L mol^{-1} cm^{-1})	λ_{max2}/nm (ϵ_2/L mol^{-1} cm^{-1})	λ_{max3}/nm (ϵ_3/L mol^{-1} cm^{-1})	ref
1[a]		339 (400)	456 (570)	this work
2[a]		366 (3940)	462 (1560)	this work
3[a]		406 (1918)	510 (2073)	16
4[a]	293 (26830)	376 (5000)	479 (4150)	this work
5[a]	326 (41250)	395 (8080)	483 (6500)	this work
6[a]	347 (52230)		532 (780)	5
7[b]	295 (38020)		544 (590)	14
8[c]	252 (2140)	320	542 (830)	2

[a] Spectra recorded in dichloromethane. [b] Spectra recorded in chloroform. [c] Spectra recorded in cyclohexane.

TABLE 2: Third-Order Nonlinear Susceptibilities γ of Compounds 4−6 Recorded in Dichloromethane

compd	concn/mol L^{-1}	$10^{34}\gamma_{micro}$/esu
4	7.8×10^{-3}	0.9 (± 0.35)
	8.9×10^{-3}	0.8 (± 0.07)
5	1.5×10^{-2}	0.85 (± 0.3)
	1.1×10^{-2}	0.76 (± 0.1)
6	1.1×10^{-2}	2.5 (±0.1)

TABLE 3: Cyclic Voltammetry Data Recorded for Compounds 1−5 and Comparison with Literature Data for 6[5], 7[14] and 8[3]

mpd	$E°_{ox}$/V vs Fc	$E°_{red}$/V vs Fc
1	0.39	
2	0.13	
3	0.14	
4	0.27	−1.22[a]
5	0.04	−1.26[a]
6		−1.21
7		−1.24
8		−1.20

[a] Not fully reversible.

For comparison, the Fe(II)/Fe(III) oxidation potentials of ferrocenylnitrile (**1**), 4-ferrocenylbenzonitrile (**2**), and 4-ferrocenylnitrobenzene (**3**) were determined using cyclic voltammetry under the same conditions. All oxidation potentials (as well as reduction potentials for the tetrazines) are presented in the Table 3. They are as expected: shifted anodically with respect to the oxidation potential of ferrocene (0.1 V vs Ag^+/Ag), which indicates a reduction of electron density on the iron atom by the effect of electron-withdrawing groups. Comparison of the oxidation potential of tetrazine **4** and **5** with related compounds **1** and **2** reveals 120 and 90 mV cathodic shifts, respectively, which demonstrates changes in intermolecular charge transfer interactions in the solution. A respectable reduction of electron withdrawing character of acceptor moieties is observed between tetrazines **4** and **5**, this latter containing an additional phenyl unit. A similar feature is observed when compounds **1** and **2** or **1** and **3** are compared. From the comparison between the oxidation potentials of **1** and **4**, it can be seen that the efficiency of the electron attracting power of the tetrazine ring is superior to the one of the cyano group, because one *single* tetrazine induces a potential shift of +0.27 V on each of *two* ferrocenes, whereas one cyano group on one *single* ferrocene induces a potential shift of +0.39 V.

Both tetrazines are reducible at moderately low potentials (−1.22 V (**4**) and −1.26 V (**5**)), substitution by ferrocene in these compounds resulting in the same shift (−0.02 V) compared to *s*-tetrazine (**8**) (−1.20 V) and 3,6-bisphenyltetrazine (**7**) (−1.24 V), respectively. However, it is noteworthy that the ferrocene has much less influence on the reduction potential of the tetrazine than the tetrazine ring has on the oxidation potential of the substituted ferrocenes. This means that the LUMO orbital in compounds **4** and **5** should be essentially centered on the tetrazine ring (see below).

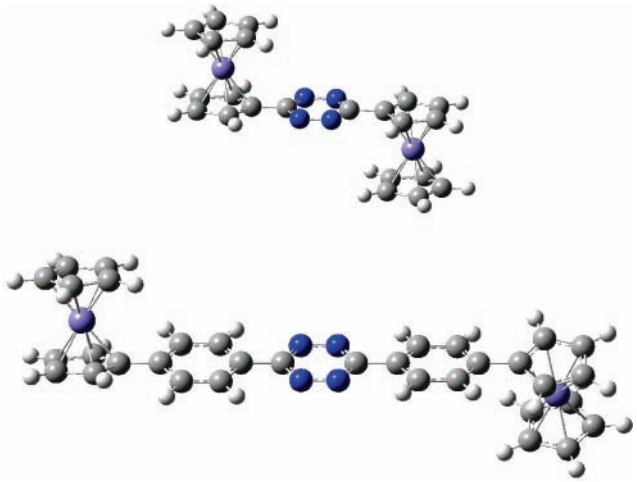

Figure 4. Optimized geometry of compounds **4** (top) and **5** (bottom).

Density Functional Theory (DFT) Calculations. Geometry optimization of both tetrazines **4** and **5** has been performed by DFT calculation (b3pw91 hybrid functional and 6-311g** basis) (Figure 4). Results indicate that although in **4** the dihedral angle between the tetrazine ring and the connected cyclopentadienyl ring is less than 1°, this angle between the ferrocene and the phenyl rings in **5** is approximately 17°. Hence, **4** can be considered as fully planar and **5** displays a clear disruption of conjugation between the central tetrazine and the phenyl rings and the peripheral ferrocenes. This variation of geometries can explain the different behaviors of tetrazines **4** and **5** toward oxidation.

Calculations performed on the ion radicals (Figure 5) confirm that the spin density in all cases is located on the tetrazine ring (radical anions) or the iron atom (radical cation). Unfortunately, the radical cation of **4** could not be obtained by the employed methods. But it is clear that the reduction potential that involves essentially the central ring should be weakly affected by the substituants. This is confirmed by the nature of the lowest unoccupied molecular orbital (LUMO) in both **4** and **5**, which is solely located on the nitrogen atoms.

Finally, TDDFT (B3LYP) calculations carried out on compounds **4** and **5** in a vacuum confirm the observed absorption spectroscopic data (Table 4). The main transitions found show three regions of absorption for each compound at ca. 350, 400 and 500 nm (two close bands) and a very small one located around 600 nm, which is the n−π* transition. It is then understandable that this transition is shadowed by the stronger MLCT band located around 500 nm. The relative positions of the band and the calculated oscillator strength both agree with the observed spectra. Inspection of the involved orbitals for the

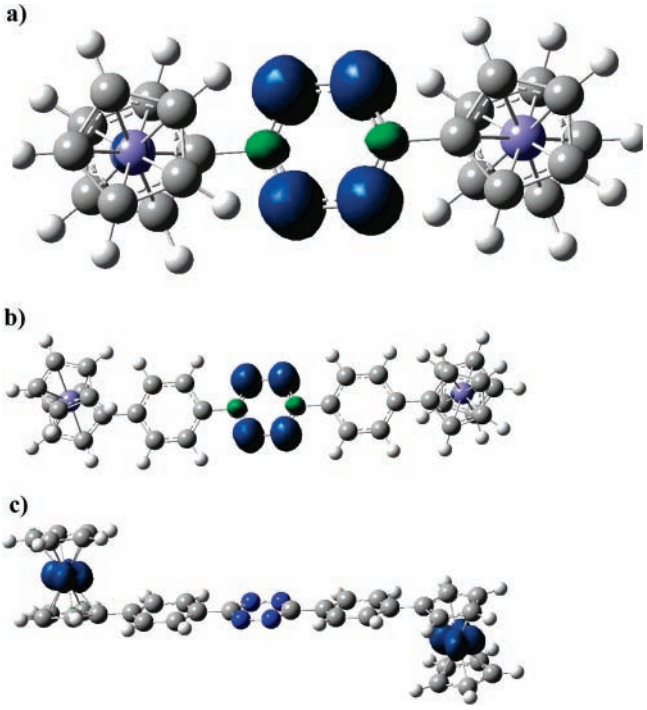

Figure 5. Spin density (isodensity at 0.004 au) for anion radicals of **4** (a), **5** (b) and the cation radical of **5** (c).

TABLE 4: Main Transitions Wavelengths and Oscillator Strengths Obtained by TDDFT (B3LYP)

4	584.23	530.18	495.93	387.17	336.36
	(0.0028)	(0.0172)	(0.0213)	(0.038)	(0.1598)
5	601.98	526.13	525.41	424.8	374.88
	(0.0033)	(0.0428)	(0.0463)	(0.3437)	(0.8667)

transition located in the UV range shows that although for **4** they are located on the tetrazine ring, for **5** they are delocalized on the adjacent phenyl rings, hence elongating the conjugation and explaining the observed bathochromic shift.

Experimental Section

Compounds **1**−**3** were prepared according to published procedure.[12,13]

Preparation of 4 and 5. To a solution of 2×10^{-3} mol of Ar−CN (0.42 g of ferrocenylnitrile (**1**) or 0.57 g of 4-ferrocenylbenzonitrile (**2**)) in 1.5 mL of absolute ethanol were added 0.032 g (1×10^{-3} mol) of powdered sulfur and 0.15 mL (3×10^{-3} mol) of freshly distilled hydrazine monohydrate. The mixture was stirred and warmed at 85 °C for 1.5 h in a closed 15 mL ACE pressure tube (25.4 mm thick wall) protected by a ***safety shield***. The vessel was cooled to room temperature and carefully ***opened under a well-ventilated hood*** (production of H_2S during the reaction). The crude dihydrotetrazine was diluted with 30 mL of absolute ethanol and then treated by an excess of isoamyl nitrite. The oxidation of dihydrotetrazines was controlled by thin layer chromatrography . After evaporation, the residue was purified by silica gel chromatography (cyclohexane:dichloromethane 1:1 v/v) to afford final tetrazines as dark pink-red colored solids (yield for two steps: 20% (**4**), 15% (**5**)).

4: ^{1}H NMR ($CDCl_3$) 5.01 (pseudo-t, $J = 2.0$ Hz, $2H_{Cp}$), 4.66 (pseudo-t, $J = 2.0$ Hz, $2H_{Cp}$), 4.14 (s, $5H_{Cp}$); ^{13}C NMR ($CDCl_3$) 181.18 (C tetrazine), 77.11, 72.33, 70.83, 70.47; IR 1505 cm^{-1}-(−C═N); *m*/*z* (ESI) 450 (M^+), 451 (MH^+), 211 (FeCN).

5: ^{1}H NMR ($CDCl_3$) 7.96 (d, $J = 8,3$ Hz, $2H_{Ph}$), 7.62 (d, $J = 8,3$ Hz, $2H_{Ph}$), 4.75 (pseudo-t, $J = 1.8$ Hz, $2H_{Cp}$), 4.45 (pseudo-t, $J = 1.8$ Hz, $2H_{Cp}$), 4.07 (s, $5H_{Cp}$); ^{13}C NMR ($CDCl_3$) 178.97 (C tetrazine), 146.06, 129.76, 126.66, 123.32, 82.53, 70.13, 69.87, 66.84; IR 1601 cm^{-1}(−C═N); *m*/*z* (ESI) 301 (FeC_6H_4CNN), 287 (FeC_6H_4CN).

Electrochemistry. The electrochemical studies were performed using an EG&G PAR 273 potentiostat, interfaced to a PC computer. Cyclic voltammograms at scan rates higher than 0.1 V s^{-1} were obtained on a homemade potentiostat equipped with a manual ohmic drop compensation system[19] The reference electrode used was an Ag electrode filled with 0.01 M $AgNO_3$. This reference electrode was checked vs ferrocene as recommended by IUPAC. In our case, $E°(Fc^+/Fc) = 0.100$ V in dichloromethane with 0.1 M TEAP. A platinum wire and a glassy carbon disk (1 mm diameter) were used respectively as counter and working electrodes. Tetrabutylammonium perchlorate was purchased from Fluka (puriss). Acetonitrile (Aldrich, 99.8%) and dichloromethane (SDS, 99.9%) were used as received. All solutions were deaerated by bubbling argon gas for a few minutes prior to electrochemical measurements.

UV−Vis Spectroscopy. A UV−vis Varian CARY 500 spectrophotometer was used. Solvents were of spectroscopic grade.

Nonlinear Optical Measurements. Third harmonic generation (THG) measurements have been performed at 1.91 μm using a hydrogen Raman shifter pumped at 1.06 μm by an 10 Hz repetition rate, 15 ns Nd^{3+}:YAG laser. Solutions of molecules **4**−**6** in chloroform were placed in an EFISH-type cell,[20] where silica windows are arranged to form a small angle prism of the investigated solution. This geometry allows for a continuous change of the interaction length and results in the obtention of THG "Maker fringes" when the cell is translated perpendicular to the incident beam. The fundamental wave was vertically polarized. THG fringes were detected by a photomultiplier, processed by a boxcar integrator and a computer. From the period and amplitude of Maker fringes, and with pure chloroform as a reference, we can infer the macroscopic $\chi^{(3)}$ values of the solution and then the microscopic γ values.

Conclusion

In this report we described spectral and electrochemical properties of two D−A−D tetrazine systems containing ferrocene as a donor unit (**4**, **5**) and a phenyl group as a π-bridge (**5**). UV−vis spectroscopic but also cyclic voltammetric studies show intramolecular charge transfer interaction in the solution, especially when there is no spacer in the molecule. The oxidation potential of Fc moieties indicates that the separation of the charge in **4** is considerably greater than in **5** in the ground state due to the presence of the phenyl linkage between the ferrocene and tetrazine moieties, which increases the electron density on the Fc units. On the other hand, UV−vis studies show an increase of facility of charge transfer due to the phenyl linkage between the ferrocene and tetrazine moieties. Both tetrazines display reduction potentials in the same range, showing a much weaker influence of the Fc substituants on the tetrazines than the other way around. Although the voltammograms are not fully reversible for compound **4**, both tetrazines constitute potential molecules for the device. Their third-order NLO properties show that the ferrocenyl group does not play a highly positive role in the optimization of γ values. However, it evidences the possible role of metal-to-ligand charge transfer on third-order hyperpolarizability values, confirming the counteractive effect of the charge transfer process already reported for quadratic nonlinear responses.

References and Notes

(1) Audebert, P.; Matsunaga, K.; Kamada, K.; Ohta, K. *Chem. Phys. Lett.* **2003**, *367*, 62.

(2) Katritzky, A. R. *Handbook of Heterocyclic Chemistry*; Pergamon Press: Oxford, U.K., 1986.

(3) Troll, T. *Electrochim. Acta* **1982**, *27* (9), 1311.

(4) Kaim, W. *Coord. Chem. Rev.* **2002**, *230*, 127.

(5) Audebert, P.; Sadki, S.; Miomandre, F.; Clavier, G.; Vernières, M. C.; Saoud, M.; Hapiot, P. *New J. Chem.* **2004**, *28*, 387.

(6) Togni, A., Hayashi, T., Eds. *Ferrocenes*; VCH Verlagsgesellschaft: Weinheim, Germany, 1995.

(7) Barlow, S.; Bunting, H.; Ringham, C.; Green, J.; Bublitz, G.; Boxer, S.; Perry, J.; Marder, S. *J. Am. Chem. Soc.* **1999**, *121*, 3715.

(8) Calabrese, J.; Cheng, L.; Green, J.; Marder, S.; Tam, W. *J. Am. Chem. Soc.* **1991**, *113*, 7227.

(9) Alain, V.; Fort, A.; Barzoukas, M.; Chen, C.; Blanchard-Desce, M.; Marder, S.; Perry, J. *Inorg. Chim. Acta* **1996**, *242*, 43.

(10) Janowska, I.; Zakrzewski, J.; Nakatani, K.; Delaire, J. *J. Organomet. Chem.* **2003**, *675*, 35.

(11) Abdel-Rahman, M. O.; Kira, M. A.; Tolba, M. N. *Tetrahedron Lett.* **1968**, 3871.

(12) Zhang, J. L.; Ch. Dong, E.; Zhi, Y. G.; Zhang, L. F. *Chin. Chem. Lett.* **2000**, *11* (2), 107.

(13) Coe, B. J.; Ch. Jones, J.; McCleverty, J. A. *J. Organomet. Chem.* **1994**, *464*, 225.

(14) Farkas, L.; Keuler, J.; Wamhoff, H. *Chem. Ber.* **1980** *113*, 2566.

(15) Waluk, J.; Spanget-Larsen, J.; Thulstrup, E. W. *Chem. Phys.* **1995**, *200*, 201.

(16) Imrie, Ch.; Dilworth, J. R.; Zheng, Y. *J. Chem. Soc., Dalton Trans*. **2001**, 2624.

(17) Cheng, L−T.; Tam, W.; Marder, S. R.; Stiegman, A. E.; Rikken, G.; Spangler, C. W. *J. Phys. Chem.* **1991**, *95*, 10643.

(18) Vance, F. W.; Hupp, J. T. *J. Am. Chem. Soc.* **1999**, *121*, 4047. Maury, O.; Viau, L.; Sénéchal, K.; Corre, B.; Guégan, J.-P.; Renouard, T.; Ledoux, I.; Zyss, J.; Le Bozec, H. *Chem. Eur. J.* **2004**, *10*, 4454.

(19) Garreau, D.; Savéant, J. M. *J. Electroanal. Chem.* **1975**, *50*, 1.

(20) Levine, B. F.; Bethea, C. G. *Appl. Phys. Lett.* **1974**, *24*, 445. Oudar, J. L. *J. Chem. Phys.* **1977**, *67*, 446.